Composites: Part B 45 (2013) 1258–1264

Contents lists available at SciVerse ScienceDirect

Composites: Part B

journal homepage: www.elsevier.com/locate/compositesb

A finite element model using a unified formulation for the analysis of viscoelastic sandwich laminates

A.J.M. Ferreira [a,*], A.L. Araújo [b], A.M.A. Neves [a], J.D. Rodrigues [c], E. Carrera [d], M. Cinefra [d], C.M. Mota Soares [b]

[a] Departamento de Engenharia Mecânica, Faculdade de Engenharia, Universidade do Porto, Rua Dr. Roberto Frias, 4200-465 Porto, Portugal
[b] IDMEC/IST, Universidade Técnica de Lisboa, Av. Rovisco Pais, 1049-001 Lisboa, Portugal
[c] INEGI, Faculdade de Engenharia, Universidade do Porto, Rua Dr. Roberto Frias, 4200-465 Porto, Portugal
[d] Departament of Aeronautics and Aerospace Engineering, Politecnico di Torino, Corso Duca degli Abruzzi, 24, 10129 Torino, Italy

ARTICLE INFO

Article history:
Received 20 April 2012
Received in revised form 17 May 2012
Accepted 18 May 2012
Available online 30 May 2012

Keywords:
A. Plates
A. Layered structures
B. Vibration
C. Finite element analysis (FEA)

ABSTRACT

In this paper we present a layerwise finite element model for the analysis of sandwich laminated plates with a viscoelastic core and laminated anisotropic face layers. The stiffness and mass matrices of the element are obtained by Carrera's Unified Formulation (CUF). The dynamic problem is solved in the frequency domain with viscoelastic frequency-dependent material properties for the core. The dynamic behaviour of the model is compared with solutions found in the literature, including experimental data.

1. Introduction

Sandwich plates with viscoelastic core are very effective in reducing and controlling vibration response of lightweight and flexible structures, where the soft core is strongly deformed in shear, due to the adjacent stiff layers. The theoretical work on constrained layer damping can be traced to DiTaranto [1] and Mead and Markus [2] for the axial and bending vibration of sandwich beams. Since then, different formulations and techniques have been reported for modelling and predicting the energy dissipation of the viscoelastic core layer in a vibrating passive constrained layer damping structure [3–5]. Other proposed formulations include thickness deformation of the core layer [6] and deal with the cases where only a portion of the base structure receives treatment [7].

Due to the high shear developed inside the core of the sandwich, equivalent single layer plate theories, even those based on higher order deformations, are not adequate to describe the behaviour of these sandwiches, also due to the high deformation discontinuities that arise at the interfaces between the viscoelastic core material and the surrounding elastic constraining layers. The usual approach to analyse the dynamic response of sandwich plates uses a layered scheme of plate and brick elements with nodal linkage. This approach leads to a time consuming spatial modelling task. To overcome these difficulties, the layerwise theory has been considered for constrained viscoelastic treatments, and most recently, Moreira et al. [8,9], among others, presented generalised layerwise formulations in this scope.

A review and assessment of various theories for modelling sandwich composites with application to sandwich beams can be found in the work of Hu et al. [10].

More recently, Araújo et al. [11–14] have presented and used for optimisation and viscoelastic material identification purposes a sandwich finite element model based on an eight nodded serendipity plate element. The viscoelastic core layer is modelled according to a higher order shear deformation theory and adjacent elastic and piezoelectric layers are modelled using the first order shear deformation theory. All materials are considered to be orthotropic, with elastic layers being formulated as laminated composite plies. Passive damping is accounted for by using the complex modulus approach, allowing for frequency dependent viscoelastic materials and active damping is incorporated through feedback control laws for co-located control. Also in this framework, Moita et al. [15] developed a simple and efficient non conforming triangular finite element where the viscoelastic core is modelled according to Reissner–Mindlin laminated plate theory and the face layers are modelled according the Kirchhoff–Love plate theory. Another sandwich plate model presented by Moita et al. [16] is based on Reddy's third order shear deformation theory for the core and

* Corresponding author.
E-mail address: ferreira@fe.up.pt (A.J.M. Ferreira).

1359-8368/$ - see front matter © 2012 Elsevier Ltd. All rights reserved.
http://dx.doi.org/10.1016/j.compositesb.2012.05.012

the face layers are also modelled according to the classical laminated plate theory. These models also contemplate hybrid active–passive damping. A similar model was also presented by Bilasse et al. [17] for non linear vibrations of sandwich plates.

In the present work the stiffness and mass matrices are obtained by Carrera's Unified Formulation (CUF), firstly proposed in [18–20] for laminated plates and shells and extended to functionally graded (FG) plates in [21–23]. The present formulation considers a displacement-based layerwise formulation, with linear expansion of displacements in each layer, with degrees of freedom u_x, u_y, u_z at each lamina interface. To the authors knowledge, it is the first time that CUF is applied to this class of problems with viscoelastic behaviour. The main advantage of the present formulation is its versatility allowing for great flexibility in the through the thickness approximations, which is an important feature in sandwich structures.

The dynamic response of the finite element model is validated using a few reference solutions from the literature.

2. Stiffness and mass matrices by the unified formulation

This section intends to detail how the stiffness and mass matrices are obtained, in order to support the relevant (nonlinear) eigenproblem, to be discussed later.

2.1. Geometry and notations for multilayered plates

Consider a laminated plate with N_l layers, where we will denote k for the layer number that starts from the bottom surface. Let x and y be the plate middle surface Ω^k coordinates. Ω_0 and Ω will denote the reference surface of the plate and of the element, respectively. Let Γ^k be the layer boundary on Ω^k. Let z and z_k be the plate and layer thickness coordinates; and $h,\ h_k$ denote plate and layer thickness, respectively. In order to compute integrals in the thickness direction, we also denote A_k as the kth-layer thickness domain. Symbols not affected by k subscript/superscript refer to the whole plate.

2.2. Displacement assumptions

The present Layerwise (LW) approach considers independent layers, where the displacement vector $\mathbf{u}^k$ is expressed in terms of the values at each laminate interface. The typical expansion for displacements is expressed as

$$\mathbf{u}^k = F_t\mathbf{u}_t^k + F_b\mathbf{u}_b^k = F_\tau\mathbf{u}_\tau^k; \quad \tau = t,b; \quad k = 1,2,\ldots,N_l \tag{1}$$

and

$$\mathbf{u}^{(k)} = [\,u_x \quad u_y \quad u_z\,]^T \tag{2}$$

where $t,\ b$ denote the top and bottom surfaces of the lamina. We are using linear functions in each layer, as follows:

$$F_b = 0.5 - \frac{1}{h^{(k)}}\left(z - \frac{z_b^{(k)} + z_t^{(k)}}{2}\right);$$
$$F_t = 0.5 + \frac{1}{h^{(k)}}\left(z - \frac{z_b^{(k)} + z_t^{(k)}}{2}\right) \tag{3}$$

The thickness for each layer is obtained as $h^{(k)} = z_t^{(k)} - z_b^{(k)}$. The quantities referred in Eq. (3) are illustrated in Fig. 1 for a 3-layered laminate.

2.3. Strain–displacement relations

Resorting to the small deformation assumptions, the in-plane (p), and out-of-plane (n) strain components $\boldsymbol{\epsilon}_p^{(k)}, \boldsymbol{\epsilon}_n^{(k)}$ are linearly related to the displacements $\mathbf{u}^{(k)}$ according to

$$\boldsymbol{\epsilon}_p^{(k)} = \mathbf{D}_p\mathbf{u}^{(k)} \tag{4}$$
$$\boldsymbol{\epsilon}_n^{(k)} = \mathbf{D}_n\mathbf{u}^{(k)} = (\mathbf{D}_{n\Omega} + \mathbf{D}_{nz})\mathbf{u}^{(k)} \tag{5}$$

The differential matrices are expressed as

$$\mathbf{D}_p = \begin{bmatrix} \frac{\partial}{\partial x} & 0 & 0 \\ 0 & \frac{\partial}{\partial y} & 0 \\ \frac{\partial}{\partial y} & \frac{\partial}{\partial x} & 0 \end{bmatrix}; \quad \mathbf{D}_n = \begin{bmatrix} \frac{\partial}{\partial z} & 0 & \frac{\partial}{\partial x} \\ 0 & \frac{\partial}{\partial z} & \frac{\partial}{\partial y} \\ 0 & 0 & \frac{\partial}{\partial z} \end{bmatrix}; \quad \mathbf{D}_{n\Omega} = \begin{bmatrix} 0 & 0 & \frac{\partial}{\partial x} \\ 0 & 0 & \frac{\partial}{\partial y} \\ 0 & 0 & 0 \end{bmatrix};$$
$$\mathbf{D}_{nz} = \begin{bmatrix} \frac{\partial}{\partial z} & 0 & 0 \\ 0 & \frac{\partial}{\partial z} & 0 \\ 0 & 0 & \frac{\partial}{\partial z} \end{bmatrix} \tag{6}$$

2.4. Hooke's law for orthotropic lamina in the material reference system

The linear elastic laminae are considered to be homogeneous. Hooke's law for the anisotropic k-lamina is written in the form $\sigma_i = C_{ij}\epsilon_j$, where the sub-indices i and j, ranging from 1 to 6, stand for the index couples 11, 22, 33, 13, 23 and 12, respectively. The material is assumed to be orthotropic. Therefore, $C_{14} = C_{24} = C_{34} = C_{64} = C_{15} = C_{25} = C_{35} = C_{65} = 0$. This implies that σ_{13}^k and σ_{23}^k depend on ϵ_{13}^k and ϵ_{23}^k only. In matrix form it can be written

$$\begin{bmatrix} \sigma_{11} \\ \sigma_{22} \\ \sigma_{12} \\ \sigma_{13} \\ \sigma_{23} \\ \sigma_{33} \end{bmatrix} = \begin{bmatrix} C_{11} & C_{12} & 0 & 0 & 0 & C_{13} \\ C_{12} & C_{22} & 0 & 0 & 0 & C_{23} \\ 0 & 0 & C_{66} & 0 & 0 & 0 \\ 0 & 0 & 0 & C_{55} & 0 & 0 \\ 0 & 0 & 0 & 0 & C_{44} & 0 \\ C_{13} & C_{23} & 0 & 0 & 0 & C_{33} \end{bmatrix} \begin{bmatrix} \epsilon_{11} \\ \epsilon_{22} \\ \epsilon_{12} \\ \epsilon_{13} \\ \epsilon_{23} \\ \epsilon_{33} \end{bmatrix} \tag{7}$$

2.5. Hooke' law for orthotropic lamina in the plate reference system

Multilayered plates are often composed by layers made up with different orientation. It is therefore of interest to write Hooke's law on the material coordinate system 1, 2, 3 into the reference coordinate system $x,\ y,\ z$. The relations between the two coordinate systems are expressed as:

$$\boldsymbol{\sigma} = \mathbf{T}\boldsymbol{\sigma}_m; \quad \boldsymbol{\epsilon}_{\boldsymbol{m}} = \mathbf{T}^T\boldsymbol{\epsilon}; \quad \boldsymbol{\sigma}_{\boldsymbol{m}} = \mathbf{C}\boldsymbol{\epsilon}_{\boldsymbol{m}} \tag{8}$$

where

$$\boldsymbol{\sigma}_{\boldsymbol{m}} = [\,\sigma_{11} \quad \sigma_{22} \quad \sigma_{12} \quad \sigma_{13} \quad \sigma_{23} \quad \sigma_{33}\,]^T \tag{9}$$

$$\boldsymbol{\epsilon}_{\boldsymbol{m}} = [\,\epsilon_{11} \quad \epsilon_{22} \quad \epsilon_{12} \quad \epsilon_{13} \quad \epsilon_{23} \quad \epsilon_{33}\,]^T \tag{10}$$

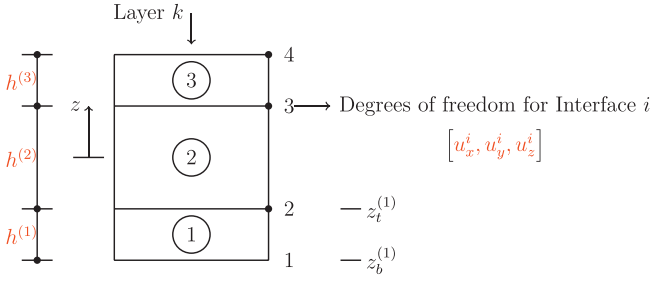

Fig. 1. A 3-layer laminate; definition of degrees of freedom at the four interfaces.

$$\boldsymbol{\sigma} = [\,\sigma_{xx} \quad \sigma_{yy} \quad \sigma_{xy} \quad \sigma_{xz} \quad \sigma_{yz} \quad \sigma_{zz}\,]^T \tag{11}$$

$$\boldsymbol{\epsilon} = [\,\epsilon_{xx} \quad \epsilon_{yy} \quad \epsilon_{xy} \quad \epsilon_{xz} \quad \epsilon_{yz} \quad \epsilon_{zz}\,]^T \tag{12}$$

and $\mathbf{T}$ denotes the matrix of direction cosines of the coordinate transformation. Using previous relations, we can finally obtain the stress–strain relations in the reference coordinate system as

$$\boldsymbol{\sigma} = \mathbf{T}\mathbf{C}\mathbf{T}^T\boldsymbol{\epsilon} = \widetilde{\mathbf{C}}\boldsymbol{\epsilon} \tag{13}$$

2.6. Viscoelastic core

For the viscoelastic core layer, the stiffness coefficients C_{ij} are complex quantities. The complex modulus approach was used in this work, according to the elastic–viscoelastic correspondence principle. In this case, the usual engineering moduli may be represented by complex quantities, considering isothermal conditions (see Araujo et al. [13] for details), as

$$\begin{aligned}
E_1^*(j\omega) &= E_1(\omega)(1+j\eta_{E_1}(\omega))\\
E_2^*(j\omega) &= E_2(\omega)(1+j\eta_{E_2}(\omega))\\
E_3^*(j\omega) &= E_3(\omega)(1+j\eta_{E_3}(\omega))\\
G_{12}^*(j\omega) &= G_{12}(\omega)(1+j\eta_{G_{12}}(\omega))\\
G_{23}^*(j\omega) &= G_{23}(\omega)(1+j\eta_{G_{23}}(\omega))\\
G_{13}^*(j\omega) &= G_{13}(\omega)(1+j\eta_{G_{13}}(\omega))\\
\nu_{12}^*(j\omega) &= \nu_{12}(\omega)(1-j\eta_{\nu_{12}}(\omega))\\
\nu_{13}^*(j\omega) &= \nu_{13}(\omega)(1-j\eta_{\nu_{13}}(\omega))\\
\nu_{23}^*(j\omega) &= \nu_{23}(\omega)(1-j\eta_{\nu_{23}}(\omega))
\end{aligned} \tag{14}$$

where E_1, E_2, E_3, G_{12}, G_{23}, G_{13} and ν_{12}, ν_{13}, ν_{23} denote storage moduli, η_{E_1}, η_{E_2}, η_{E_3}, $\eta_{G_{12}}$, $\eta_{G_{23}}$, $\eta_{G_{13}}$ and $\eta_{\nu_{12}}$, $\eta_{\nu_{13}}$, $\eta_{\nu_{23}}$ are the corresponding material loss factors, ω represents the angular frequency of vibration and $j = \sqrt{-1}$ is the imaginary unit.

2.7. Finite element interpolations

Following standard finite element method (FEM) approximations, the unknown variables in the element domain are expressed in terms of their values at the element nodes. According to the isoparametric description, displacements are expressed as

$$\mathbf{u}_\tau^k = N_i\mathbf{q}_{\tau i}^k \quad (i = 1, 2, \ldots, N_n) \tag{15}$$

where

$$\mathbf{q}_{\tau i}^k = \begin{bmatrix} q_{u_x\tau i}^k & q_{u_y\tau i}^k & q_{u_z\tau i}^k \end{bmatrix}^T \tag{16}$$

Here, N_n is the number of element nodes, N_i are the shape functions and $\mathbf{q}_{\tau i}^k$ are nodal variables.

The assumed displacement field is first introduced in the expression for the strains, leading to the following expressions:

$$\boldsymbol{\varepsilon}_p^k = \mathbf{D}_p\mathbf{u}^k = \mathbf{D}_p\big(F_\tau\mathbf{u}_\tau^k\big) \tag{17}$$

$$\boldsymbol{\varepsilon}_n^k = \mathbf{D}_n\mathbf{u}^k = (\mathbf{D}_{n\Omega} + \mathbf{D}_{nz})\big(F_\tau\mathbf{u}_\tau^k\big) = \mathbf{D}_{n\Omega}\big(F_\tau\mathbf{u}_\tau^k\big) + F_{\tau_z}\mathbf{u}_\tau^k \tag{18}$$

In which the notation $F_{\tau_z} = \frac{\partial F_\tau}{\partial z}$ has been introduced. Being the base functions F_τ independent of x and y, the strains can now be written as

$$\boldsymbol{\varepsilon}_p^k = F_\tau\mathbf{D}_p(N_i\mathbf{I})\mathbf{q}_{\tau i}^k; \quad \boldsymbol{\varepsilon}_n^k = F_\tau\mathbf{D}_{n\Omega}(N_i\mathbf{I})\mathbf{q}_{\tau i}^k + F_{\tau_z}N_i\mathbf{q}_{\tau i}^k \tag{19}$$

in which $\mathbf{I}$ is the identity matrix. By introducing the strain–displacement relations along with Hooke's law, the internal virtual strain energy can be expressed via the Principle of Virtual Displacements (PVDs) statement as

$$\begin{aligned}
\delta L_{int}^k = &\int_\Omega \delta\mathbf{q}_{\tau i}^{kT}\mathbf{D}_p^T(N_i\mathbf{I})\widetilde{\mathbf{C}}_{pp}^k\Big[\int_{A_k}(F_\tau F_s)dz\Big]\mathbf{D}_p(N_j\mathbf{I})\mathbf{q}_{sj}^k d\Omega\\
&+\int_\Omega \delta\mathbf{q}_{\tau i}^{kT}\mathbf{D}_p^T(N_i\mathbf{I})\widetilde{\mathbf{C}}_{pn}^k\Big[\int_{A_k}(F_\tau F_s)dz\Big]\mathbf{D}_{n\Omega}(N_j\mathbf{I})\mathbf{q}_{sj}^k d\Omega\\
&+\int_\Omega \delta\mathbf{q}_{\tau i}^{kT}\mathbf{D}_p^T(N_i\mathbf{I})\widetilde{\mathbf{C}}_{pn}^k\Big[\int_{A_k}(F_\tau F_{s_z})dz\Big]N_j\mathbf{q}_{sj}^k d\Omega\\
&+\int_\Omega \delta\mathbf{q}_{\tau i}^{kT}\mathbf{D}_{n\Omega}^T(N_i\mathbf{I})\widetilde{\mathbf{C}}_{np}^k\Big[\int_{A_k}(F_\tau F_s)dz\Big]\mathbf{D}_p(N_j\mathbf{I})\mathbf{q}_{sj}^k d\Omega\\
&+\int_\Omega \delta\mathbf{q}_{\tau i}^{kT}\mathbf{D}_{n\Omega}^T(N_i\mathbf{I})\widetilde{\mathbf{C}}_{nn}^k\Big[\int_{A_k}(F_\tau F_s)dz\Big]\mathbf{D}_{n\Omega}(N_j\mathbf{I})\mathbf{q}_{sj}^k d\Omega\\
&+\int_\Omega \delta\mathbf{q}_{\tau i}^{kT}\mathbf{D}_{n\Omega}^T(N_i\mathbf{I})\widetilde{\mathbf{C}}_{nn}^k\Big[\int_{A_k}(F_\tau F_{s_z})dz\Big]N_j\mathbf{q}_{sj}^k d\Omega\\
&+\int_\Omega \delta\mathbf{q}_{\tau i}^{kT}N_i\widetilde{\mathbf{C}}_{np}^k\Big[\int_{A_k}(F_{\tau_z}F_s)dz\Big]\mathbf{D}_p(N_j\mathbf{I})\mathbf{q}_{sj}^k d\Omega\\
&+\int_\Omega \delta\mathbf{q}_{\tau i}^{kT}N_i\widetilde{\mathbf{C}}_{nn}^k\Big[\int_{A_k}(F_{\tau_z}F_s)dz\Big]\mathbf{D}_{n\Omega}(N_j\mathbf{I})\mathbf{q}_{sj}^k d\Omega\\
&+\int_\Omega \delta\mathbf{q}_{\tau i}^{kT}N_i\widetilde{\mathbf{C}}_{nn}^k\Big[\int_{A_k}(F_{\tau_z}F_{s_z})dz\Big]N_j\mathbf{q}_{sj}^k d\Omega
\end{aligned} \tag{20}$$

where Ω represents the domain of the finite element, and $\widetilde{\mathbf{C}}^k$ have been introduced in compact form in Eq. (13). To notice once again that subscripts s and j have been used for the finite values of unknown variables while subscripts τ and i have been introduced for their virtual variations. As usual in two dimensional analysis, the integration in the thickness direction can be made beforehand by introducing the following layer integrals

$$\Big(\widetilde{\mathbf{Z}}_{pp}^{k\tau s}, \widetilde{\mathbf{Z}}_{pn}^{k\tau s}, \widetilde{\mathbf{Z}}_{np}^{k\tau s}, \widetilde{\mathbf{Z}}_{nn}^{k\tau s},\Big) = \Big(\widetilde{\mathbf{C}}_{pp}^k, \widetilde{\mathbf{C}}_{pn}^k, \widetilde{\mathbf{C}}_{np}^k, \widetilde{\mathbf{C}}_{nn}^k\Big)E_{\tau s} \tag{21}$$

$$\begin{aligned}
&\Big(\widetilde{\mathbf{Z}}_{pn}^{k\tau s_z}, \widetilde{\mathbf{Z}}_{nn}^{k\tau s_z}, \widetilde{\mathbf{Z}}_{np}^{k\tau_z s}, \widetilde{\mathbf{Z}}_{nn}^{k\tau_z s}, \widetilde{\mathbf{Z}}_{nn}^{k\tau_z s_z}\Big)\\
&\quad = \Big(\widetilde{\mathbf{C}}_{pn}^k E_{\tau s_z}, \widetilde{\mathbf{C}}_{nn}^k E_{\tau s_z}, \widetilde{\mathbf{C}}_{np}^k E_{\tau_z s}, \widetilde{\mathbf{C}}_{nn}^k E_{\tau_z s}^k, \widetilde{\mathbf{C}}_{nn}^k E_{\tau_z s_z}\Big)
\end{aligned} \tag{22}$$

where

$$(E_{\tau s}, E_{\tau s_z}, E_{\tau_z s}, E_{\tau_z s_z}) = \int_{A_k}(F_\tau F_s, F_\tau F_{s_z}, F_{\tau_z}F_s, F_{\tau_z}F_{s_z})dz \tag{23}$$

Note that F_τ and F_s have been introduced before for each layer as F_b and F_t in Eq. (3).

Eq. (20) can be written as

$$\delta L_{int}^k = \delta\mathbf{q}_{\tau i}^{kT}\mathbf{K}^{k\tau sij}\mathbf{q}_{sj}^k \tag{24}$$

where $\mathbf{K}^{k\tau sij}$ represents the kth layer stiffness matrix, defined as

$$\begin{aligned}
\mathbf{K}^{k\tau sij} = &\lhd\mathbf{D}_p^T(N_i\mathbf{I})\Big[\widetilde{\mathbf{Z}}_{pp}^{k\tau s}\mathbf{D}_p(N_j\mathbf{I}) + \widetilde{\mathbf{Z}}_{pn}^{k\tau s}\mathbf{D}_{n\Omega}(N_j\mathbf{I}) + \widetilde{\mathbf{Z}}_{pn}^{k\tau s_z}N_j\Big]\\
&+\mathbf{D}_{n\Omega}^T(N_i\mathbf{I})\Big[\widetilde{\mathbf{Z}}_{np}^{k\tau s}\mathbf{D}_p(N_j\mathbf{I}) + \widetilde{\mathbf{Z}}_{nn}^{k\tau s}\mathbf{D}_{n\Omega}(N_j\mathbf{I}) + \widetilde{\mathbf{Z}}_{nn}^{k\tau_z s}N_j\Big]\\
&+N_i\Big[\widetilde{\mathbf{Z}}_{np}^{k\tau_z s}\mathbf{D}_p(N_j\mathbf{I}) + \widetilde{\mathbf{Z}}_{nn}^{k\tau_z s}\mathbf{D}_{n\Omega}(N_j\mathbf{I}) + \widetilde{\mathbf{Z}}_{nn}^{k\tau_z s_z}N_j\Big]\rhd_\Omega
\end{aligned} \tag{25}$$

Symbol $\lhd\ldots\rhd_\Omega$ denotes integration on the finite element domain, Ω.

To notice that the matrix $\mathbf{K}^{k\tau sij}$ is made by triplicate products of 3×3 arrays, so that $\mathbf{K}^{k\tau sij}$ is itself a 3×3 array. Such an array is the fundamental nucleus of finite element matrices related to PVD applications. The nine terms of $\mathbf{K}^{k\tau sij}$ can be explicitly presented as:

$$\begin{aligned}
K_{xx}^{k\tau sij} = &\widetilde{Z}_{pp11}^{k\tau s}\lhd N_{i,x}N_{j,x}\rhd_\Omega + \widetilde{Z}_{pp16}^{k\tau s}\lhd N_{i,y}N_{j,x}\rhd_\Omega\\
&+\widetilde{Z}_{pp16}^{k\tau s}\lhd N_{i,x}N_{j,y}\rhd_\Omega + \widetilde{Z}_{pp66}^{k\tau s}\lhd N_{i,y}N_{j,y}\rhd_\Omega + \widetilde{Z}_{nn55}^{k\tau_z s_z}\lhd N_iN_j\rhd_\Omega\\
K_{xy}^{k\tau sij} = &\widetilde{Z}_{pp12}^{k\tau s}\lhd N_{i,x}N_{j,y}\rhd_\Omega + \widetilde{Z}_{pp26}^{k\tau s}\lhd N_{i,y}N_{j,y}\rhd_\Omega\\
&+\widetilde{Z}_{pp16}^{k\tau s}\lhd N_{i,x}N_{j,x}\rhd_\Omega + \widetilde{Z}_{pp66}^{k\tau s}\lhd N_{i,y}N_{j,x}\rhd_\Omega + \widetilde{Z}_{nn45}^{k\tau_z s_z}\lhd N_iN_j\rhd_\Omega\\
K_{xz}^{k\tau sij} = &\widetilde{Z}_{pn13}^{k\tau s_z}\lhd N_{i,x}N_j\rhd_\Omega + \widetilde{Z}_{pn36}^{k\tau s_z}\lhd N_{i,y}N_j\rhd_\Omega\\
&+\widetilde{Z}_{nn55}^{k\tau_z s}\lhd N_iN_{j,x}\rhd_\Omega + \widetilde{Z}_{nn45}^{k\tau_z s}\lhd N_iN_{j,y}\rhd_\Omega
\end{aligned}$$

$$
\begin{aligned}
K_{yx}^{k\tau sij} &= \widetilde{Z}_{pp12}^{k\tau s} \lhd N_{i,y} N_{j,x} \rhd_\Omega + \widetilde{Z}_{pp16}^{k\tau s} \lhd N_{i,x} N_{j,x} \rhd_\Omega \\
&\quad + \widetilde{Z}_{pp26}^{k\tau s} \lhd N_{i,y} N_{j,y} \rhd_\Omega + \widetilde{Z}_{pp66}^{k\tau s} \lhd N_{i,x} N_{j,y} \rhd_\Omega + \widetilde{Z}_{nn45}^{k\tau_z s_z} \lhd N_i N_j \rhd_\Omega \\
K_{yy}^{k\tau sij} &= \widetilde{Z}_{pp22}^{k\tau s} \lhd N_{i,y} N_{j,y} \rhd_\Omega + \widetilde{Z}_{pp26}^{k\tau s} \lhd N_{i,x} N_{j,y} \rhd_\Omega \\
&\quad + \widetilde{Z}_{pp26}^{k\tau s} \lhd N_{i,y} N_{j,x} \rhd_\Omega + \widetilde{Z}_{pp66}^{k\tau s} \lhd N_{i,x} N_{j,x} \rhd_\Omega + \widetilde{Z}_{nn44}^{k\tau_z s_z} \lhd N_i N_j \rhd_\Omega \\
K_{yz}^{k\tau sij} &= \widetilde{Z}_{pn23}^{k\tau s_z} \lhd N_{i,y} N_j \rhd_\Omega + \widetilde{Z}_{pn36}^{k\tau s_z} \lhd N_{i,x} N_j \rhd_\Omega \\
&\quad + \widetilde{Z}_{nn45}^{k\tau_z s} \lhd N_i N_{j,x} \rhd_\Omega + \widetilde{Z}_{nn44}^{k\tau_z s} \lhd N_i N_{j,y} \rhd_\Omega \\
K_{zx}^{k\tau sij} &= \widetilde{Z}_{nn55}^{k\tau s_z k} \lhd N_{i,x} N_j \rhd_\Omega + \widetilde{Z}_{nn45}^{k\tau s_z k} \lhd N_{i,y} N_j \rhd_\Omega \\
&\quad + \widetilde{Z}_{np13}^{k\tau_z s} \lhd N_i N_{j,x} \rhd_\Omega + \widetilde{Z}_{np36}^{k\tau_z s} \lhd N_i N_{j,y} \rhd_\Omega \\
K_{zy}^{k\tau sij} &= \widetilde{Z}_{nn45}^{k\tau s_z k} \lhd N_{i,x} N_j \rhd_\Omega + \widetilde{Z}_{nn44}^{k\tau s_z k} \lhd N_{i,y} N_j \rhd_\Omega \\
&\quad + \widetilde{Z}_{np23}^{k\tau_z s} \lhd N_i N_{j,y} \rhd_\Omega + \widetilde{Z}_{np36}^{k\tau_z s} \lhd N_i N_{j,x} \rhd_\Omega \\
K_{zz}^{k\tau sij} &= \widetilde{Z}_{nn55}^{k\tau sk} \lhd N_{i,x} N_{j,x} \rhd_\Omega + \widetilde{Z}_{nn45}^{k\tau sk} \lhd N_{i,y} N_{j,x} \rhd_\Omega \\
&\quad + \widetilde{Z}_{nn45}^{k\tau sk} \lhd N_{i,x} N_{j,y} \rhd_\Omega + \widetilde{Z}_{nn44}^{k\tau sk} \lhd N_{i,y} N_{j,y} \rhd_\Omega + \widetilde{Z}_{nn33}^{k\tau_z s_z} \lhd N_i N_j \rhd_\Omega
\end{aligned} \tag{26}
$$

According to CUF [18–20], the mass matrix (independent of the frequency) components are explicitly obtained as

$$
\begin{aligned}
M_{11}^{k\tau sij} &= m_{\tau s}^k \lhd N_i N_j \rhd_\Omega \\
M_{12}^{k\tau sij} &= 0 \\
M_{13}^{k\tau sij} &= 0 \\
M_{21}^{k\tau sij} &= 0 \\
M_{22}^{k\tau sij} &= m_{\tau s}^k \lhd N_i N_j \rhd_\Omega \\
M_{23}^{k\tau sij} &= 0 \\
M_{31}^{k\tau sij} &= 0 \\
M_{32}^{k\tau sij} &= 0 \\
M_{33}^{k\tau sij} &= m_{\tau s}^k \lhd N_i N_j \rhd_\Omega
\end{aligned} \tag{27}
$$

where

$$
m_{\tau s}^k = \int_{A_k} \rho^k F_\tau F_s dz
$$

and ρ^k denotes the specific mass for each layer k.

3. Equations of motion

The equations of motion for the plate are obtained by applying the extended Hamilton's principle, using a nine node Lagrangian plate element with 12 mechanical degrees of freedom per node (3displacements × 4 interfaces)

$$
\mathbf{M}\ddot{\tilde{\mathbf{q}}} + \mathbf{K}(\omega)\tilde{\mathbf{q}} = \mathbf{f} \tag{28}
$$

where $\tilde{\mathbf{q}}$, and $\ddot{\tilde{\mathbf{q}}}$, are displacement degrees of freedom and corresponding accelerations, respectively. $\mathbf{M}$ and $\mathbf{K}(\omega)$ are the real mass matrix and complex frequency dependent stiffness matrix for the plate, respectively, and $\mathbf{f}$ is the externally applied load vector.

Assuming harmonic vibrations, the final equilibrium equations are given in the frequency domain by:

$$
[\mathbf{K}(\omega) - \omega^2 \mathbf{M}]\widetilde{\mathbf{Q}} = \mathbf{F} \tag{29}
$$

where $\mathbf{F}(\omega) = \mathcal{F}(\mathbf{f}(t))$ is the Fourier transform of the time domain force history $\mathbf{f}(t)$ and $\widetilde{\mathbf{Q}}(\omega) = \mathcal{F}(\tilde{\mathbf{q}}(t))$ is the Fourier transform of the time domain displacement vector $\tilde{\mathbf{q}}(t)$.

For the free vibration problem the equations of motion reduce to the following non-linear eigenvalue problem due to the frequency dependent nature of the stiffness matrix:

$$
\left[\mathbf{K}(\omega) - \lambda_n^* \mathbf{M}\right]\widetilde{\mathbf{Q}}_n = \mathbf{0} \tag{30}
$$

where $\widetilde{\mathbf{Q}}_n$ is a complex eigenvector and λ_n^* is the associated complex eigenvalue, which can be written as:

Table 1
Natural frequencies [Hz] for the undamped rectangular sandwich plate.

n	Experimental [26]	FEM [26]	Rikards et al. [24]	Araujo et al. [13]	Present (4 × 4 Q9)	(8 × 4 Q9)	(12 × 10 Q9)
1	–	23	23.4	23.5	23.28	23.27	23.26
2	45	44	45.4	44.8	44.91	44.63	44.60
3	69	69	72.2	71.7	70.93	70.93	70.27
4	78	78	81.6	79.5	83.04	80.09	79.90
5	92	90	95.9	92.5	91.97	91.72	91.08
6	129	123	133.7	126.5	128.90	126.27	125.51
7	133	126	134.2	126.8	139.28	129.83	128.85
8	152	143	152.2	150.7	151.62	151.62	145.16
9	169	162	156.8	170.7	171.56	171.36	165.16
10	177	172	190.9	173.0	181.46	174.74	173.29

$$
\lambda_n^* = \lambda_n(1 + j\eta_n) \tag{31}
$$

and $\lambda_n = \omega_n^2$ is the real part of the complex eigenvalue and η_n is the corresponding modal loss factor.

The non-linear eigenvalue problem is solved iteratively, and the iterative process is considered to have converged when:

$$
\frac{\|\omega_i - \omega_{i-1}\|}{\omega_{i-1}} \leqslant \epsilon \tag{32}
$$

where ω_i and ω_{i-1} are current and previous iteration values for the real part of the particular eigenfrequency of interest, respectively, and ϵ is the convergence tolerance.

4. Applications

In this paper we present comparative results for natural frequencies and modal loss factors with reference numerical and experimental results.

4.1. Sandwich plates

4.1.1. Undamped sandwich

A symmetric and simply supported rectangular sandwich plate with aluminium face layers and a soft orthotropic core is considered [24,26]. The plate in-plane dimensions $(a \times b)$ are 1.829 m × 1.219 m, the thickness for the face layers is 0.406×10^{-3} m, and for the core is 0.635×10^{-2} m. The aluminium face layers are isotropic with elastic properties $E = 7.023 \times 10^4$ MPa, $\nu = 0.3$ and material density $\rho = 2.82 \times 10^3$ kg/m^3. The orthotropic soft core is characterised by the following properties (principal material direction 1 is aligned with the x direction):

$$
E_1 = E_2 = 137 \text{ MPa},\ G_{12} = 45.7 \text{ MPa},\ G_{13} = 137 \text{ MPa},\ G_{23} = 52.7 \text{ MPa},\ \nu_{12} = 0.5
$$

and $\rho = 124.1$ kg/m^3.

We compare the present results with FEM analysis by Araujo et al. [13], that employed Serendipity elements, using a Mindlin-like theory for the faces, and a higher-order approach for the core. We also compare with 6-node FEM results by Rikards et al. [24] (using laminated superelements formed by superposition of plate elements for each layer), and experimental results from [26], as reported in [24]. Comparative results for the first ten natural frequencies are presented in Table 1, using various Q9 meshes. A very good agreement can be observed between the present numerical results and the reference numerical and experimental ones.

4.1.2. Damped sandwich

A non-symmetric square simply supported sandwich plate with a thick damped core is considered [24,27]. The material properties and geometry of the plate are characterised by non-dimensional

Table 2
Modal loss factors for the square damped sandwich plate.

Vibration mode		FEM [27]	Rikards et al. [24]	Araujo et al. [13]	Present (4 × 4 Q9)	(8 × 8 Q9)	(12 × 12 Q9)
m	n						
1	1	0.373	0.350	0.368	0.352	0.353	0.353
1	2	0.273	0.173	0.272	0.247	0.248	0.248
1	3	0.189	0.160	0.188	0.160	0.167	0.167

quantities. The plate in-plane dimensions are $(a \times a)$ with $a = 100$, the thickness of the face layers are 0.4 and 0.28, and the thickness of the core layer is 4. The face layers are isotropic with elastic properties $E = 10^5$, $\nu = 0.3$ and material density $\rho = 1$. The isotropic soft core is characterised by the following non-dimensional properties: $G = 1$, $\nu = 0.3$, $\rho = 0.5$, and $\eta_G = 0.5$ (material loss factor associated with shear modulus).

We compare the present results with FEM analysis by Araujo et al. [13], that employed Serendipity elements, using a Mindlin-like theory for the faces, and a higher-order approach for the core. We also compare with 6-node FEM results by Rikards et al. [24] (using laminated superelements formed by superposition of plate elements for each layer), and Sadasiva and Nakra [27]. Comparative results for the first three modal loss factors and frequencies are presented in Tables 2 and 3, respectively, using various Q9 meshes for both present and reported [24,27] results, where a good agreement can be observed. The approximate nature of the energy method used by Rikards et al. [24] to calculate the modal loss factor might explain the observed deviations.

Table 6
Maxwell series terms at 27 °C of the 3 M ISD112 viscoelastic material [29].

i	Δ_i	Ω_i (rad/s)
1	0.746	468.7
2	3.265	4742.4
3	43.284	71532.5

Table 3
Frequencies (Hz) for the square damped sandwich plate.

Vibration mode		Araujo et al. [13]	Present (4 × 4 Q9)	(8 × 8 Q9)	(12 × 12 Q9)
m	n				
1	1	0.011	0.0111	0.0111	0.0111
1	2	0.020	0.0211	0.0210	0.0210
1	3	0.034	0.0377	0.0365	0.0364

Table 4
Verification of dynamic characteristics for the sandwich beam. Frequencies f_n in (Hz).

Mode n	$f_n^{(exp)}$ [25]	$f_n^{(FEM)}$ [25]	$\eta_n^{(exp)}$ [25]	$\eta_n^{(FEM)}$ [25]	Present f_n(8 × 2 Q9)	η_n	f_n(10 × 4 Q9)	η_n
$\nu_{13} = \nu_{23} = \nu_{12} = 0.3$ for the skins								
1	16	16	0.12	0.13	17.0316	0.1095	17.039	0.1092
2	100	99	0.22	0.22	104.4976	0.1848	104.5322	0.1843
3	268	271	0.26	0.25	288.7436	0.2104	288.6668	0.2097
4	496	510	0.26	0.28	496.7389	0.2728	495.2132	0.2725
$\nu_{13} = \nu_{23} = \nu_{12} = 0.0$ for the skins								
1	16	16	0.12	0.13	16.4004	0.1179	16.4003	0.1179
2	100	99	0.22	0.22	100.6279	0.1993	100.6161	0.1992
3	268	271	0.26	0.25	277.7424	0.2266	277.4800	0.2265
4	496	510	0.26	0.28	525.4678	0.2644	523.6329	0.2641

Table 5
Natural frequencies (Hz) and associated loss factors corresponding to the first six vibration modes of the sandwich plate with a constant complex core modulus, where the core's loss factor is $\eta_c = 0.5$ [29].

Trindade et al. [29]		Analytical [30]		Present (4 × 4 Q9)		8 × 8 Q9		12 × 12 Q9	
f_n	η_n	f_n	η_n	f_n	η_n	f_n	η_n	f_n	η_n
SSSS									
58.0	0.170	60.3	0.190	58.6323	0.1853	58.6094	0.1852	58.6082	0.1852
113.8	0.193	115.4	0.203	112.8628	0.2048	112.2867	0.2049	112.2535	0.2049
129.5	0.192	130.6	0.199	127.8021	0.2016	127.0450	0.2019	127.0013	0.2020
177.2	0.172	178.7	0.181	174.5079	0.1848	173.4775	0.1859	173.4180	0.1860
194.6	0.169	195.7	0.174	195.9840	0.1756	190.1897	0.1793	189.8335	0.1795
232.9	0.156	–	–	233.7982	0.1612	226.1713	0.1655	225.7038	0.1658
CCCC									
87.4	0.189	87.4	0.189	85.1698	0.1923	85.0548	0.1924	85.0505	0.1924
148.9	0.164	148.9	0.165	146.5786	0.1684	144.6418	0.1703	144.5534	0.1704
170.3	0.153	169.9	0.154	167.4410	0.1574	164.8201	0.1599	164.6948	0.1601
223.9	0.139	223.9	0.139	220.6600	0.1427	216.7321	0.1457	216.5612	0.1459
241.1	0.134	241.0	0.134	252.2491	0.1297	233.9649	0.1407	233.1593	0.1413
291.3	0.118	289.8	0.118	305.3447	0.1139	281.0635	0.1253	279.9708	0.1260

Table 7
Linear vibration characteristics corresponding to the first four vibration modes of the sandwich plate with 3 M ISD112 frequency dependent core at 27 °C [29], for $\omega = \omega_0$.

	[29]			Present (4 × 4 Q9)			(8 × 8 Q9)			12 × 12 Q9		
	ω_0 (rad/s)	f_n (Hz)	η_n	ω_0 (rad/s)	f_n (Hz)	η_n	ω_0 (rad/s)	f_n (Hz)	η_n	ω_0 (rad/s)	f_n (Hz)	η_n
SSSS	314.84	53.77	0.213	314.0751	53.6872	0.2355	313.9563	53.6659	0.2354	313.9500	53.6648	0.2354
	622.18	110.31	0.272	612.2826	108.4740	0.2909	608.8928	107.8791	0.2908	608.6974	107.8449	0.2908
	712.09	126.72	0.283	697.6239	123.9977	0.2968	693.1220	123.2110	0.2968	692.8626	123.1657	0.2968
	992.11	176.97	0.289	970.4160	172.9414	0.3079	963.7652	171.8744	0.3086	963.3807	171.8128	0.3087
CCCC	481.58	83.01	0.246	467.1247	80.3021	0.2495	466.3763	80.1849	0.2496	466.3443	80.1804	0.2496
	839.07	146.61	0.258	823.2952	143.6186	0.2622	811.0424	141.6222	0.2634	810.4542	141.5311	0.2635
	967.88	168.92	0.257	948.4801	165.2845	0.2607	931.7486	162.5891	0.2625	930.9136	162.4605	0.2627
	1285.48	225.27	0.270	1263.5253	221.0142	0.2733	1238.4071	216.9794	0.2754	1237.2478	216.8068	0.2757

4.2. Sandwich beam

We consider now a clamped-free sandwich beam example from Barkanov et al. [25]. The beam has dimensions: width = 0.05 m, length = 0.3 m, and thickness of layers: $h_1 = 0.0012$ m, $h_2 = 0.0001016$ m, $h_3 = 0.0008$ m. The external layers are made of aluminium 2024-T6 with the following properties: $E = 64$ GPa, $\nu = 0.32$, and $\rho = 2695$ kg/m^3. The beam is clamped on the left side and free elsewhere. The dynamic characteristics such as its eigenfrequencies and corresponding loss factors have been determined from numerical experiments using a complex eigenvalues method and the following material properties of the 3 M damping polymer ISD-112:

$$\begin{aligned} &G = 4.759 - 0.9266/z + 2.405z^2 \quad \text{(MPa)} \\ &\text{with} \quad z = 0.1918 + 0.0005148f \\ &\eta_G = \eta_E = 1.385 - 0.03673z - 0.01342/z \\ &\text{with} \quad z = 0.01 + 0.0006306f \end{aligned} \tag{33}$$

where $f = \frac{\omega}{2\pi}$, and z is not related to thickness coordinate. Poisson's ratio and density for the viscoelastic core are $\nu = 0.49$ and $\rho = 1000$ kg/m^3, respectively.

We use several Q9 meshes to compare frequencies and modal loss factors with results by Barkanov et al. [25]. We present two sets of results, one set with Poisson's ratios of the skins equal to 0.3, and another set with zero Poisson's ratios, also for the skins. As seen in Table 4, the second set presents very close results to those of [25]. This might be explained with the fact that we are modelling a beam and comparing our results with solutions based on beam theory, and also due to the presence of Poisson thickness locking [28] in the skins.

4.3. A sandwich plate with frequency-dependent viscoelastic core

A rectangular sandwich plate of in-plane dimensions 348 mm × 304.8 mm is made of two face layers with equal thickness of 0.762 mm and a viscoelastic core with a thickness of 0.254 mm. Both simply supported (SSSS) and clamped (CCCC) boundary conditions are considered. The material of the face layers is isotropic with Young modulus $E = 68.9$ GPa, Poisson's ratio $\nu = 0.3$ and mass density $\rho = 2740$ kg/m^3.

We consider two different materials for the viscoelastic core. The first material is a polymer represented by a constant viscoelastic model with $E = 2.67008$ MPa, $\nu = 0.49$, $\rho = 999$ kg/m^3 and constant loss factor $\eta = 0.5$. Results for the first six natural frequencies and modal loss factors are presented in Table 5.

The second material is the 3 M ISD112 which has a mass density of $\rho = 1600$ kg/m^3 and a Poisson's ratio of $\nu = 0.5$, and its shear modulus is frequency dependent and represented by the generalised Maxwell model [29]:

$$G^*(\omega) = G_0\left(1 + \sum_{i=1}^{n} \frac{\Delta_i \omega}{\omega - j\Omega_i}\right) \tag{34}$$

where G_0 represents the static shear modulus and $(\Delta_i,\ \Omega_i)$ the Maxwell parameters obtained by master curves fitting [29].

The 3 M ISD112 core is considered at 27 °C. The static shear modulus at this temperature is $G_0 = 0.5 \times 10^6$ Pa [29] and the corresponding Maxwell series terms (Δ_i, Ω_i) involved in the frequency dependent shear modulus are given in Table 6. The results for the first four natural frequencies and modal loss factors are presented in Table 7 for $\omega = \omega_0$, where ω_0 is the natural frequency obtained considering $\omega = 0$ in Eq. (30), following [17].

We use several Q9 meshes to compare with results by Trindade et al. [27], that used 3D cores but thin plate faces. For simply-supported plates, the results shown in Tables 5 and 7 are excellent. For clamped supports, the results show deviation of 3%. This can perhaps be explained by the fact that our layerwise approach considers 3D theory for every layer, not only for the cores, as in [29].

5. Conclusions

A new sandwich layerwise plate finite element model has been developed via a Unified Formulation for the analysis of the dynamic response of plate structures with passive damping. The complex modulus approach was used for the viscoelastic core material, along with the solution of a non linear eigenvalue problem, allowing for frequency dependent material data. The 3D constitutive equations were applied to all laminate layers. The developed nine node finite element model presents a good behaviour with passive damping, when compared to reference solutions. The response of the model has also been compared with experimental data available in the literature, showing excellent agreement.

Acknowledgements

The authors thank the financial support of FCT, through POCTI and POCI (2010)/FEDER. In particular the support of LAETA to project Composites in Mechanical Design and the support to PTDC/EME-PME/120830/2010 is gratefully acknowledged. The authors also acknowledge the kind support of FCT to Project PTDC/EME-PME/109116/2008.

References

[1] DiTaranto RA. Theory of vibratory bending for elastic and viscoelastic layered finite-length beams. ASME J Appl Mech 1965;32:881–6.
[2] Mead DJ, Markus S. The forced vibration of a three-layer, damped sandwich beam with arbitrary boundary conditions. AIAA J 1969;10:163–75.
[3] Rao DK. Frequency and loss factors of sandwich beams under various boundary conditions. Int J Mech Eng Sci 1978;20:271–8.
[4] Yan MJ, Dowell EH. Governing equations of vibrating constrained-layer damping sandwich plates and beams. ASME J Appl Mech 1972;39:1041–6.

[5] Rao MD, He S. Dynamic analysis and design of laminated composite beams with multiple damping layers. AIAA J 1993;31:736–45.
[6] Douglas BE, Yang JCS. Transverse compressional damping in the vibratory response of elastic-viscoelastic beams. AIAA J 1978;16:925–30.
[7] Lall AK, Asnani NT, Nakra BC. Damping analysis of partially covered sandwich beams. J Sound Vib 1988;123:247–59.
[8] Moreira RAS, Rodrigues JD, Ferreira AJM. A generalized layerwise finite element for multi-layer damping treatments. Comput Mech 2006;37:426–44.
[9] Moreira RAS, Rodrigues JD. A layerwise model for thin soft core sandwich plates. Comput Struct 2006;84:1256–63.
[10] Hu H, Belouettar S, Potier-Ferry M, Daya EM. Review and assessment of various theories for modeling sandwich composites. Compos Struct 2008;84(3):282–92.
[11] Araújo AL, Mota Soares CM, Mota Soares CA. Finite element model for hybrid active-passive damping analysis of anisotropic laminated sandwich structures. J Sandwich Struct Mater 2010;12(4):397–419.
[12] Araújo AL, Mota Soares CM, Mota Soares CA, Herskovits J. Optimal design and parameter estimation of frequency dependent viscoelastic laminated sandwich composite plates. Compos Struct 2010;92:2321–7.
[13] Araújo AL, Mota Soares CM, Mota Soares CA. A viscoelastic sandwich finite element model for the analysis of passive, active and hybrid structures. Appl Compos Mater 2010;17:529–42.
[14] Araújo AL, Martins P, Mota Soares CM, Mota Soares CA, Herskovits J. Damping optimisation of hybrid active-passive sandwich composite structures. Adv Eng Software 2012;46:69–74.
[15] Moita JS, Araújo AL, Martins P, Mota Soares CM, Mota Soares CA. A finite element model for the analysis of viscoelastic sandwich structures. Comput Struct 2011;89:1874–81.
[16] Moita JS, Araújo AL, Martins P, Mota Soares CM, Mota Soares CA. Analysis of active-passive plate structures using a simple and efficient finite element model. Mech Adv Mater Struct 2011;18:159–69.
[17] Bilasse M, Azrar L, Daya EM. Complex modes based numerical analysis of viscoelastic sandwich plates vibrations. Comput Struct 2011;89:539–55.
[18] Carrera E. Developments, ideas, and evaluations based upon reissner's mixed variational theorem in the modelling of multilayered plates and shells. Appl Mech Rev 2001;54:301–29.
[19] Carrera E. Evaluation of layer-wise mixed theories for laminated plate analysis. AIAA J 1998(36):830–9.
[20] Erasmo Carrera. Theories and finite elements for multilayered plates and shells: a unified compact formulation with numerical assessment and benchmarking. Arch Comput Methods Eng 2003;10:215–96.
[21] Brischetto S, Carrera E. Advanced mixed theories for bending analysis of functionally graded plates. Comput Struct 2010;88(23-24):1474–83.
[22] Brischetto S. Classical and mixed advanced models for sandwich plates embedding functionally graded cores. J Mech Mater Struct 2009;4:13–33.
[23] Carrera E, Brischetto S, Robaldo A. Variable kinematic model for the analysis of functionally graded material plates. AIAA J 2008;46:194–203.
[24] Rikards R, Chate A, Barkanov E. Finite element analysis of damping the vibrations of laminated composites. Comput Struct 1993;47:1005–15.
[25] Barkanov E, Skukis E, Petitjean B. Characterisation of viscoelastic layers in sandwich panels via an inverse technique. J Sound Vib 2009;327:402–12.
[26] Alam N, Asnani NT. Vibration and damping analysis of multilayered rectangular plates with constrained viscoelastic layers. J Sound Vib 1984;97:597–614.
[27] Sadasiva Rao YV, Nakra BC. Vibrations of unsymmetrical sandwich beams and plates with viscoelastic cores. J Sound Vib 1974;34:309–26.
[28] Bischoff M, Ramm E. On the physical significance of higher order kinematic and static variables in a three-dimensional shell formulation. Int J Solids Struct 2000;37:6933–60.
[29] Trindade M, Benjeddou A, Ohayon R. Modeling of frequency dependent viscoelastic materials for active-passive vibration damping. J Vib Acoust 2000;122(2):169–74.
[30] Johnson C, Kienholz D. Finite element prediction of damping in structures with constrained viscoelastic layers. Am Inst Aeronaut Astronaut J 1982;20: 128–490.